Synthesis and Characterization of Segmented Liquid Crystalline Polymers with the Azo Group in the Main Chain

Domenico Acierno,[†] Eugenio Amendola,[‡] Valeria Bugatti,[§] Simona Concilio,[§] Loris Giorgini,[||] Pio Iannelli,*[,§] and Stefano P. Piotto[§]

Dipartimento di Ingegneria dei Materiali e della Produzione, Università di Napoli, P. le Tecchio, I-80125 Napoli, Italy, Institute for Composite Materials and Biomaterials (IMCB)- CNR, P. le Tecchio, I-80125 Napoli, Italy, Dipartimento di Ingegneria Chimica ed Alimentare, Università di Salerno, via Ponte Don Melillo, I-84084 Fisciano (Salerno), Italy, and Dipartimento di Chimica Industriale e dei Materiali, Università di Bologna, viale Risorgimento 4, 40136 Bologna, Italy

Received April 7, 2004; Revised Manuscript Received June 15, 2004

ABSTRACT: The synthesis of 4′-hydroxyphenyl(4-hydroxy-3-allyl)azobenzene is reported. The molecule is mesogenic and it can be used for preparing nematic main-chain segmented polymers. The nematic phase is the result of the effect of the side allyl group which, while it destabilizes the crystalline phase, does not affect the occurring of the nematic order. In the crystalline state, a large hexagonal unit cell containing five to six chains is observed for polymers with longer flexible spacer in the chain. Chloroform solutions and thin films of polymers absorb in the UV−visible range, at approximately 332 and 439 nm, corresponding to the $\pi \rightarrow \pi^*$ and $n \rightarrow \pi^*$ electronic transitions of azoaromatic chromophores, respectively. Under appropriate UV irradiation we have obtained the photoisomerizations trans−cis and cis−trans, which are fully reversible in the case of solutions. In the solid state a photostationary state is reached.

1. Introduction

Nematic liquid crystalline polymers (PCLs) can be easily oriented by extrusion from the molten state. The high degree of orientation may be "frozen" by a fast quench at a temperature lower than the glass transition temperature. This macro-oriented state cannot be considered to be in a thermodynamic equilibrium, and the orientation is lost at the macroscopic level, when samples are heated on the glass transition. A way to stabilize the orientation is to chemically cross-link the system immediately after the preparation of the manufact. It is then possible to completely freeze the orientation by varying the cross-link density, to improve the mechanical properties especially at high temperatures. If the cross-link degree is small, the polymeric chains possess a sufficient mobility to undergo the isotropization, which occurs at higher temperature than in the virgin sample, because the LC phase stability has been increased. The process is associated with a strong contraction and it is completely reversible. This material behaves as a thermal-mechanical engine (actuator system). This is the case for the polymer bearing the allylbiphenol as mesogenic unit and having the following formula:[1,2]

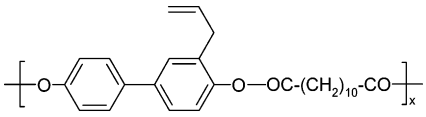

P10

In the last few years a large amount of papers have been reported on LCPs bearing azo-groups in the mesogenic unit.[3−11] These contributions regard mainly the synthesis and the characterization of *side-chain* LCPs. Because of the quite low activation energy of the cis−trans transition, these polymeric materials have been widely considered for their potential application in the field of photoswitching and optical storage.[12,13] Among these studies, some applications regarding the destabilization of LC order accompanying the cis−trans isomerization have been considered for reversible photoswitchable system, from transparent to opaque state.[14−16] Particularly interesting is the induced macroscopic deformation of cross-linked thin films of liquid crystalline azobenzene compounds, when irradiated by linearly polarized light.[17] The azobenzene compounds used are liquid crystalline monomers bearing one or two acrylate units, which are cross-linked by thermal polymerization. In this way, thin films with good mechanical properties are obtained. When irradiated with a linearly polarized light at 366 nm, films bend in a direction perpendicular to the plane of vibration of polarized light. The result is a photoactuator system, which transform a light impulse in a mechanical response. The contraction is fully reversible when films are irradiated with visible light with a wavelength longer than 540 nm.

In this paper we will report on the synthesis and the characterization of a new class of *main-chain* segmented LCPs having the following formula:

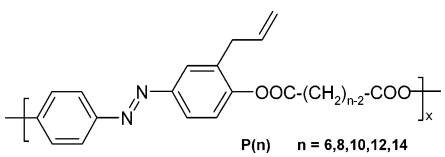

P(n) n = 6,8,10,12,14

Our attention will be focused particularly on the characterization of UV−vis behavior of this new class of polymers, both in solution and solid state, to evaluate

* Corresponding author. E-mail: piannelli@unisa.it.
[†] Università di Napoli.
[‡] Institute for Composite Materials and Biomaterials (IMCB)-CNR.
[§] Università di Salerno.
[||] Università di Bologna.

10.1021/ma049319k CCC: $27.50
Published on Web 07/30/2004

Scheme 1

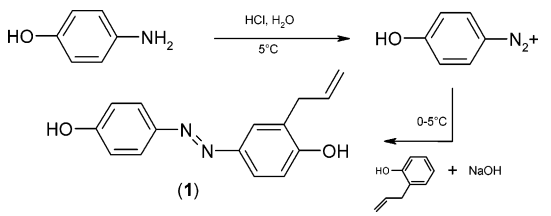

Scheme 2

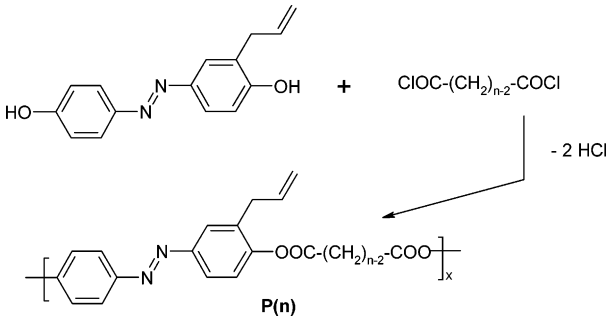

the feasibility of this new class of nematic polymers as materials for photoactuator devices.

2. Experimental Section

2.1. Synthetic Procedures. All reagents and solvents were purchased from Aldrich and Carlo Erba and they were used without further purification. *N*,*N*-Dimethylformamide (DMF) was refluxed on calcium hydride, distilled in a vacuum, and stored on 4 Å molecular sieves. α,ω-Alkoxydicarboxylic dichloride was prepared following the standard procedure, by refluxing the correspondent dicarboxylic acid in thionyl chloride for 6 h followed by distillation under vacuum.

2.1.1. Synthesis of 4′-Hydroxyphenyl(4-hydroxy-3-allyl)azobenzene (1) [See Scheme 1]. Monomer 4′-hydroxyphenyl(4-hydroxy-3-allyl)azobenzene (**1**) was synthesized according to the classic scheme of diazotization−coupling reaction, as illustrated in Scheme 1. The procedure was the following: 5.0 g of *p*-aminophenol (0.0458 mol) was suspended in a solution containing 40 mL of water and 10 mL of HCl 37%w (0.122 mol). The solution was cooled at 0−5 °C in a water−ice bath. Under stirring, a solution obtained dissolving 3.48 g of sodium nitrite (0.0504 mol) in 10 mL of water (solution A) was added slowly. Stirring at low temperature was continued for 20 min after the addition of the nitrite solution was completed, obtaining, at the end, a suspension of the diazonium salt. Separately, a solution containing 7.38 g of NaOH (0.1846 mol) in 40 mL of water with 6.15 g of 2-allylphenol (0.0458 mol) was prepared (solution B). Solution A was added dropwise to solution B, under stirring at 5 °C. The system was left reacting for 20 min more. Then the final solution was added slowly to 700 mL of acid water (HCl) and a red-orange precipitate of the azo-compound formed. The precipitate was filtered and washed with water containing a little amount of sodium hydrogen carbonate (pH = 8). The red solid was dried under vacuum, and final recrystallization from boiling *n*-octane (500 mL) gave pure **1** as a red-orange crystalline material. Final yields ranged between 50% and 60%.

The proton resonance data are in agreement with the expected values: (acetone-d_6): δ (ppm) = 7.78 (m, 2H); 7.71 (s,1H); 7.64 (d, 1H); 6.99 (m, 3H); 6.07 (m, 1H); 5.07 (m, 2H); 3.47 (m, 2H) T_m = 144.3 °C, ΔH_m = 135 J/g.

2.1.2. Polymer Synthesis [See Scheme 2]. **P(*n*)** were synthesized by solution polycondensation reaction, following Scheme 2, by using stoichiometric amount of monomer **1** and of the dichlorides of aliphatic dicarboxylic acids. The procedure was the following [**P(10)** taken as a representative example]: 0.302 g of monomer **1** (0.00119 mol) was dissolved in 5.0 mL of DMF with 0.0941 g of pyridine (0.00119 mol). Then 0.284 g of sebacoyl chloride was dissolved in 1.0 mL of DMF and slowly added to the previous solution under stirring. The system was left to react for 18 h at room temperature, and then the slightly pink solution was slowly poured in water and the resulting solid was filtered. The product was washed with water, dried under vacuum, and purified by precipitation from chloroform solution with *n*-heptane.

The proton resonance data are in agreement with the expected values: for example, **P(10)** ($CDCl_3$): δ (ppm) = 7.91 (d, 2H); 7.82 (m, 2H); 7.22 (m, 3H); 5.97 (m, 1H); 5.13 (t, 2H); 3.40 (m, 2H); 2.62 (m, 4H); 1.80 (m, 4H); 1.37 (m, 8H).

2.2. Characterization. Thermal measurements were performed by a DSC-7 Perkin-Elmer calorimeter under nitrogen flow at 10 °C/min rate.

Polarized optical microscopy was performed by a Jenapol microscope fitted with a Linkam THMS 600 hot stage.

X-ray diffraction spectra were recorded using a flat camera with a sample-to-film distance of 140 mm (Ni-filtered Cu Kα radiation). High-temperature X-ray diffraction patterns were collected using a modified Linkam THMS 600 hot stage. The Fujifilm MS 2025 imaging plate and a Fuji bioimaging analyzer system, model BAS-1800, were used for recording and digitizing the diffraction patterns.

^{1}H NMR spectra were recorded with a Bruker DRX/400 spectrometer. Chemical shifts are reported relative to the residual solvent peak (chloroform-*d*: H = 7.26).

A Waters 150-C ALC/SEC instrument was used for SEC analysis (size exclusion cromatography), equipped with six 300 × 7.5 mm^2 columns (Waters Styragel HT3, HT4, HT5, HT6, 500 Å, and 400 Å) and a Jasco 875 UV detector set at 254 nm (polystyrene as standard and chloroform as solvent, at 1 mL/min and 30 °C).

UV absorption spectra of the samples were recorded at 25 °C in $CHCl_3$ solution on a Perkin-Elmer Lambda 19 spectrophotometer. The spectral region 650−240 nm was investigated by using a cell path length of 1 cm. Azobenzene chromophore concentration of 4.6×10^{-5} mol·L^{-1} was used.

Photoisomerization experiments were carried out at 25 °C on samples in chloroform solution (3 mL with absorbance ∼0.4 at irradiation wavelength of 366 nm) using the following experimental setup: the emission from a 150 W medium-pressure Hg lamp (Hanau), filtered by a 366 or 434 nm interference filter (Balzer) with a ±5 nm bandwidth, was guided by a 3 mm × 50 cm quartz fiber on top of a magnetically stirred solution of the sample, in a 10 mm quartz cell placed within the UV spectrophotometer. The isomerization kinetics were monitored by measuring the 340 nm absorbance after several irradiation times until the photostationary state was reached.

Amorphous thin films have been prepared by spin-coating solutions of polymers in chloroform (1% w/w) over clean fused silica substrates. Then, films were dried under vacuum at 25 °C overnight to eliminate the residual solvent. The film thickness was regulated to give UV−visible spectra with maximum absorbance between 0.7 and 1.5 units, depending on the procedure conditions. By inspection with a cross polarized optical microscope, the virgin films were optically isotropic. The experiments of photoisomerization of azoaromatic units in isotropic and nematic thin solid films (irradiated area of 0.5 cm^2) were carried out at room temperature by using the same Hg lamp, filters, and quartz fiber of the experiments in solution until the occurrence of stable UV-visible signals, recorded after several times of irradiation with a Perkin-Elmer Lambda 19 spectrophotometer.

3. Discussion

3.1. Thermal Characterization. Polarized optical microscopy and DSC analysis show that all polymers **P(*n*)** exhibit enantiotropic liquid-crystalline phase. The X-ray diffraction pattern recorded within the thermal stability range of the LC phase of **P(6)**, **P(8)**, and **P-(10)** is consistent with the nematic phase. It is characterized by an equatorial halo with a *d*-spacing of 4.1 Å, and no Bragg diffraction is observed for lattice distances

Table 1. Isotropization Temperature and Enthalpy of P(*n*)

n	T_i (°C)	ΔH_i (J/g)	M_w ($\times 10^3$)	*c* (Å)[a]
6	152.4	8.5	8.0	19.3
8	131.7	8.8	16.2	21.6
10	117.4	10.3	19.4	22.4
12	104.4	11.1[b]	10.8	25.6
14	97.7	12.4[b]	8.6	26.3

[a] "*c*" axis length, as obtained from the meridian spots detected in the diffraction pattern. [b] Evaluated by integration of the anisotropization peak.

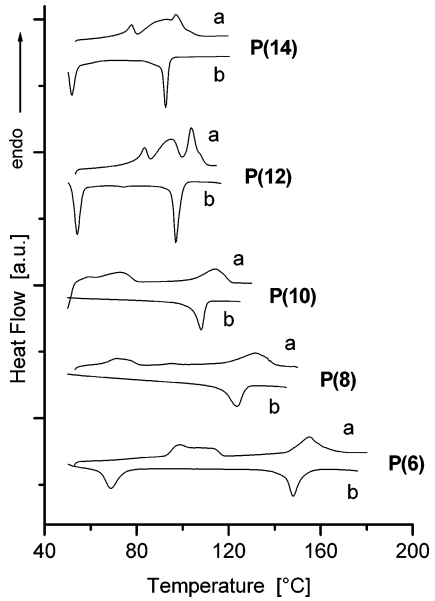

Figure 1. Calorimetric traces of virgin samples of **P(*n*)**, as obtained from the synthesis: (a) first heating run; (b) first cooling run.

lower approximately 50 Å. Thermodynamic data and DSC traces of virgin samples of **P(*n*)** as obtained from the synthesis are given in Table 1 and Figure 1, respectively. According to what was observed for analogous polymers, the allyl-substituent disturbs the packing of the polymer chains, thus melting temperature is quite low while the nematic phase is still stable to be detected. For $n = 12$ and 14, melting and isotropization transitions overlap to some extent, and the thermal characterization could be performed in the cooling run, which allows the separation of the two peaks.

By repeating heating and cooling runs on the same samples, calorimetric curves are unaffected, showing that allyl unit is stable and spontaneous thermal cross-linking does not occur under mild conditions. Thermal cross-linking is promoted only by an activator agent like *tert*-butylperoxibenzoate.

3.2. X-ray Diffraction Analysis. The polymers, as obtained from the synthesis, are in a poorly crystallized state, which is, in general, little improved by annealing (see below). The X-ray diffraction analysis, performed on both virgin and fiber samples, shows the occurrence of a mesophase stable at room temperature, the structure of which depends on the length of flexible segment along the chain.

For **P(6)** and **P(8)**, the mesophase stable at room temperature is a smectic C type phase, quenched during the cooling process. As an example, the diffraction pattern of **P(8)** is shown in Figure 2a: the two out-of-order meridian 00*l* diffractions are clearly detectable. They correspond to the *d*-spacing of the smectic layer

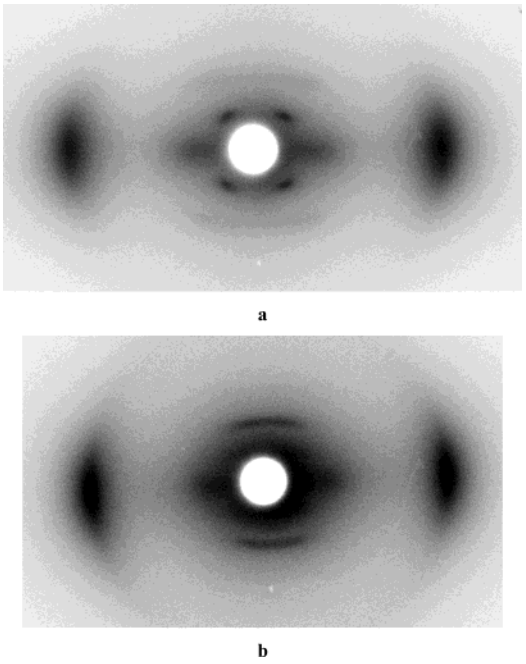

Figure 2. (a) Fiber X-ray diffraction pattern of **P(6)** and **P-(8)**, quenched smectic C type mesophase; (b) Fiber X-ray diffraction pattern of **P(10)**, quenched nematic (cybotactic) phase.

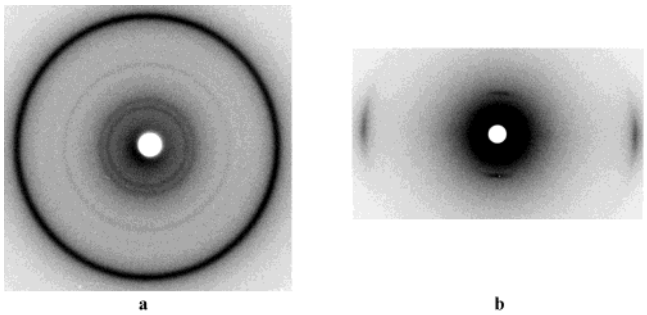

Figure 3. X-ray diffraction patterns of **P(12)**: (a) powder sample annealed at 70 °C for 30 min, crystalline phase; (b) fiber sample, quenched smectic type phase.

periodicity (21.6 Å), which is consistent with the repeating unit length along the chain. The equatorial spot corresponds to the nematic *d*-spacing of 4.1 Å.

The room-temperature mesophase of **P(10)** resembles very much the nematic phase quenched during extrusion (Figure 2b). There is a layer spot close to the meridian, but only the first order is detectable.

P(12) and **P(14)** represent a different case. According to that reported by some of us on analogous class of PCLs bearing side allyl unit,[1] the length of flexible spacer along the chain strongly affect the molecular packing in the solid state. Particularly, long flexible segment improve mobility and the self-organization of several chains to form bundles. Such bundles may arrange, by the effect of an adequate annealing, in a hexagonal array. This is particularly evident in Figure 3.a, which shows that the hexagonal phase can be obtained by annealing virgin samples of the polymer. The two-dimensional hexagonal cell having cell parameters $a = b = 12.6$ Å and $\gamma = 120°$ accounts well the diffraction pattern in Figure 3a (see Table 2). The observed density of 1.07 g cm^{-3} suggest that this large unit cell should contain five/six chains with a calculated density of 1.05/1.21 g cm^{-3}, respectively. For fiber

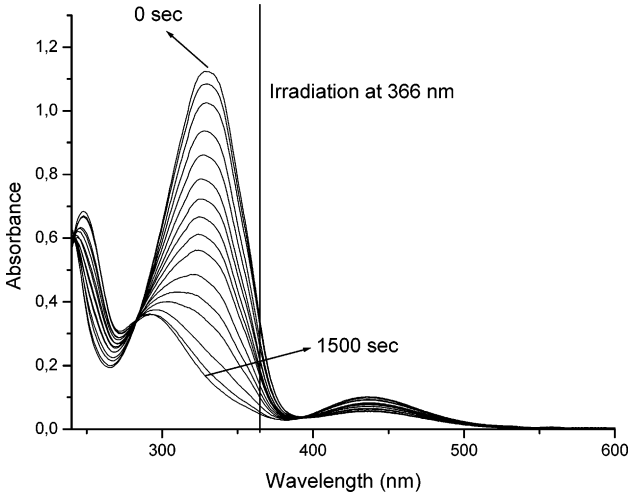

Figure 4. UV−visible spectra of **P(8)** in chloroform solution at 25 °C, with different irradiation times, at 366 nm.

Table 2. Bragg Indices of Diffraction Rings (Figure 3a): P(12)

hkl	*d*-spacing (Å) obsd	*d*-spacing (Å) calcd	intensity (on visual base)
100, 010, 1$\bar{1}$0	10.9	10.9	medium
110, 1$\bar{2}$0, 2$\bar{1}$0	6.27	6.30	weak
200, 020, 2$\bar{2}$0	5.43	5.46	very weak
120, 1$\bar{3}$0, 210, 2$\bar{3}$0, 3$\bar{1}$0, 3$\bar{2}$0	4.09	4.12	very very strong

samples, the stable mesophase at room temperature is similar to that shown by **P(10)**, but with sharper spots in the diffraction pattern (see Figure 3b). This corresponds to have larger domains.

About the layer thickness, it is equal to the length of chain in the case of **P(6)** and **P(8)**, while it is half part in the other cases. This suggests that for polymers **P(10)**−**P(14)** chains are shifted each other by half the chain length and form an aggregate that packs in a perfect hexagonal array in the case of **P(12)** and **P(14)**. Moreover, the repeating unit length of all polymers does not correspond to that calculated for the most extended conformation: for example, for **P(14)** we observe a *d*-spacing of 26.3 Å against the calculated value of 30.5 Å. This may be accounted for either a not all-trans aliphatic sequence along the chain or the occurrence of reciprocal tilting of the rigid and the flexible moiety along the chain.

The liquid crystalline phase stable at high temperature is the nematic.

3.3. UV Absorption and Photochromic Properties in Solution. The UV−visible spectra of polymers, in chloroform solution, are qualitatively independent of the length of flexible segment along the chain and only depend on the active azo-containing unit, which is the same for all polymers. The UV absorption spectra in $CHCl_3$ solution of **P(8)** in trans configuration (Figure 4, not irradiated sample), in the 240−650 nm region, showed two bands centered around 332 and 439 nm, related respectively to the $\pi \rightarrow \pi^*$ and $n \rightarrow \pi^*$ electronic transitions of the azobenzene chromophore.[18] UV spectra data are given in Table 3.

On irradiation of **P(8)** solution in correspondence of the first $\pi \rightarrow \pi^*$ electronic transition, azobenzene chromophores undergo a trans-to-cis photoisomerization process. Correspondingly, shape, intensity and position of the UV absorption bands change (Figure 4). Indeed the UV spectra recorded at different irradiation times

Table 3. UV Spectra of P(8) at 25 °C $CHCl_3$ Solution[a]

sample	n → p* transition λ_{max}	n → p* transition ϵ_{max}	$\pi \rightarrow$ p* transition λ_{max}	$\pi \rightarrow$ p* transition $\epsilon_{max} \times 10^{-3}$
trans-**P(8)**	439	1200	332	24.2
cis-**P(8)**	435	1700	298	7.1

[a] λ_{max} and ϵ_{max} are expressed in nm and $L \cdot mol^{-1} \cdot cm^{-1}$, respectively; ϵ_{max} for the cis sample is calculated at the photostationary state (approximately 90% in mol of cis isomer).

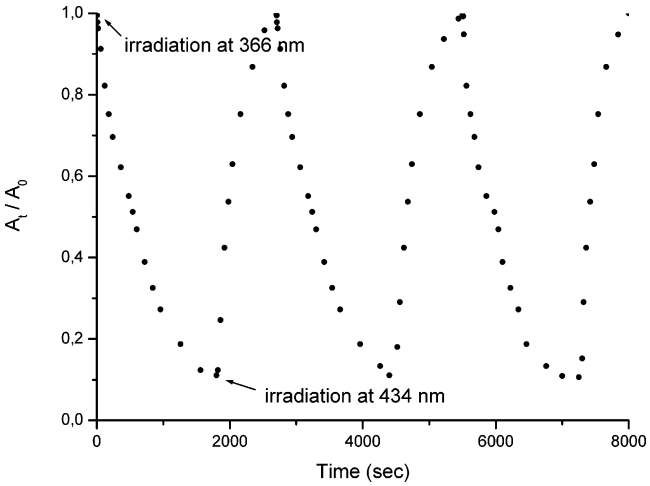

Figure 5. A_t/A_o absorption at 340 nm of **P(8)** in chloroform solution as a function of irradiation time at 366 and 434 nm, for several cycles of photoirradiation.

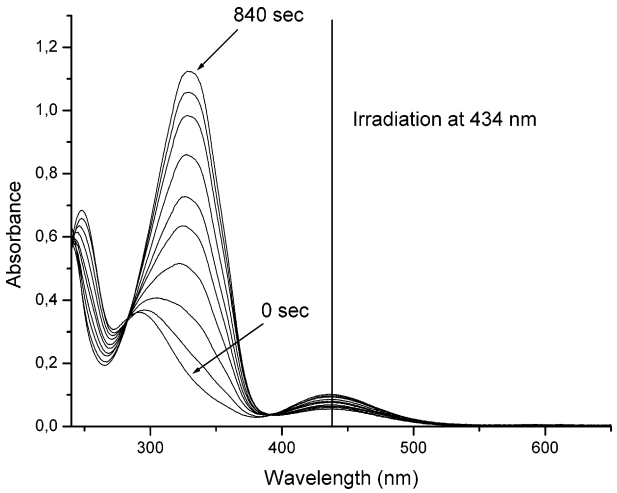

Figure 6. UV spectra of **P(8)** at different irradiation times at 434 nm in chloroform solution at 25 °C.

are characterized by the presence of two isosbestic points at about 283 and 392 nm, thus confirming that only two absorbing species, namely cis and trans isomers of the azobenzene group, are present in solution and that in these bland conditions the functionality of allyl groups are not reactive.

Photoisomerization kinetics were investigated at 25 °C on chloroform solutions, having absorbance lower than 0.4 at the irradiation wavelength. Experiments were performed by irradiation at 366 nm while monitoring the 340 nm absorbance until a photostationary state was reached, as reported in Figure 6. Kinetic data were fitted by the equation

$$\ln[(A_o - A_\infty)/(A_t - A_\infty)] = \kappa_{exp} t$$

where A_o, A_t, and A_∞ are the 340 nm absorbance at time

0, t, and ∞, respectively.[19] Trans-to-cis photoisomerization rate constant, κ_{exp}, as measured at 25 °C on chloroform solution of **P(8)**, is 1.8×10^{-4} s^{-1}. Experimental and calculated data are in very good agreement. In fact, the obtained photoisomerization rate constant linearly depends on the light intensity at the irradiation wavelength (I_λ) [according to equation: $\kappa_{exp} = 2.303 I_\lambda (\epsilon_{cis}\Phi_{cis} + \epsilon_{trans}\Phi_{trans})$,[19] where Φ_{cis} and Φ_{trans} are the quantum yields for cis−trans and trans−cis photoisomerizations, respectively], as measured by a iron−oxalate actinometry method[20] (14.0×10^{-8} mol of photons in 1 min on 3 mL of solution at 366 nm). Keeping the sample in dark for 48 h, the content of trans azobenzene of **P(8)** was completely recovered.

When irradiated at 434 nm, the 340 nm absorbance of cis-isomerized sample steadily increases up to the starting value before irradiation, thus confirming the reversibility of the photoisomerization process (Figures 5 and 6). In this case also, the process obeys a first-order kinetic. This result clearly indicates homogeneous photochromic behavior for *trans*- and *cis*-azobenzene chromophores in the polymer sample. Accordingly, the photoisomerization rate constants do not depend on the extent of isomerization, i.e., the presence of adjacent azobenzene moieties in either the trans or the cis configuration does not affect the photoisomerization kinetics.

Cis-to-trans photoisomerization rate constant, as measured at 25 °C on chloroform solution of **P(8)**, is 2.1×10^{-2} s^{-1}, with an irradiation intensity of Hg lamp at 434 nm of $3{,}6 \times 10^{-8}$ mol of photon/min on 3 mL of solution at 434 nm, measured by the same iron−oxalate actinometry method.[20] The much higher rate constant value for the cis-to-trans isomerization reaction with respect to the reverse process has to be attributed not to the different irradiation intensities of the lamp at the two wavelengths (14.0×10^{-8} mol of photon/min at 366 nm and 3.6×10^{-8} mol of photon/min at 434 nm) but to the different molar absorption extinction coefficients and quantum yields of photoisomerization of cis and trans isomers at the above wavelengths.

The recorded A_∞/A_o value (approx 0.10) in solution did not show a large dependence on the nature of the investigated sample, analogously to what observed for other azobenzene containing polymers.[21−24]

However, it is worth noting that the value of the trans → cis photoisomerization rate for **P(8)**, with chromophores in the main chain, appears 1 order of magnitude lower than those previously reported, in analogous conditions, for side-chain azobenzene chromophores-containing polymers, thus indicating that the macromolecular backbone has the tendency to depress the isomerization process.

The complete reversibility (fatigue resistance properties) of the UV spectra of **P(8)** in Figure 5, after several cycles of photoirradiation at 366 and 434 nm, seems to be promising in the photoresponsive systems field.

3.4. UV Absorption and Photochromic Properties of Film Samples. The UV−vis spectra and photochromic properties of synthesized polymers have been investigated also in solid state, as thin films prepared by spin-coating chloroform solution of polymers (1% w/w) over fused silica substrates. By inspection with a cross polarized optical microscope, the virgin films are optically isotropic. The UV−vis absorption spectra of **P(8)** in amorphous state is reported in Figure 7. It is interesting to observe that the spectra of nonirradiated samples in solution (Figure 4) are very similar to those in isotropic solid state, and that the positions of relative bands do not show any significant shift.

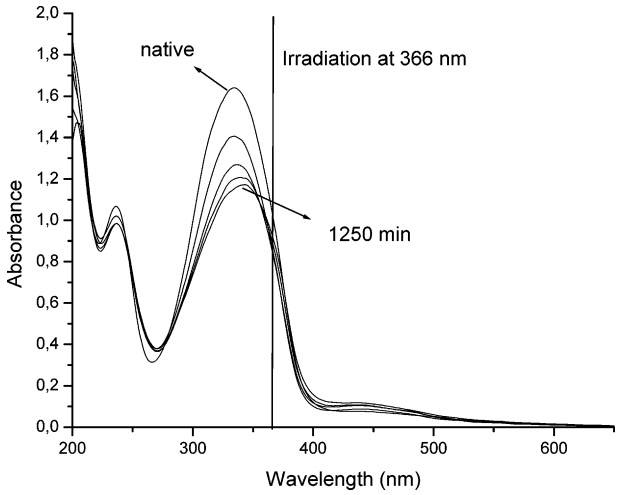

Figure 7. UV−visible spectra of **P(8)** film sample at 25 °C, at different irradiation times at 366 nm (from top to bottom: 60, 200, 380, and 1250 min of irradiation).

Under UV irradiation at 366 nm (Figure 7), the isotropic film of **P(8)** shows a typical spectral variation: the absorbance at 331 nm successively decreases with the exposure time, as a consequence of the trans-to-cis photoisomerization, which can be proved by the increase of absorbance at ∼450 nm. The remarkable lower decrease of A_t/A_o, observed by comparing the bulk−polymer with polymeric diluted solution, suggests that the photoisomerization rate, and the relative conversion in the photochemical process are substantially lower in the glassy state than in solution. Similar results were found for several polyamides[25,26] and polyureas[27,28] containing azobenzene residues in the backbone, and they were attributed to the reduced mobility of the chromophores below T_g.

When, after an irradiation for 1250 min, the photostationary state was reached, the intensity of the absorbance of trans-isomer continuously decreases, but the maximum wavelength of $\pi \rightarrow \pi^*$ electronic transition presents a significant red-shift to 342 nm, and the absorption band becomes broader. The origin of the red-shift has been attributed to an antiparallel arrangement of the chromophores as electric dipoles (J-type aggregation).[29]

The presence of these J-aggregates could have a strong influence on the reversibility of photochemical process in the solid state. In fact, under irradiation at 434 nm, the absorbance of a cis-isomerized sample steadily increases, but it never reaches the starting value of the virgin film any more (Figure 8). Moreover, the absorption wavelength of the trans-isomer presents a shift from ∼ 340 to 350 nm, and the symmetry of the absorption band changes. This further red-shift suggests the appearance of J-aggregations of trans-isomer of azobenzene chromophores also after an irradiation at 434 nm.

These processes might be due to the reorganization of the azoaromatic chromophores during the longer time of the trans−cis and cis−trans isomerizations, caused by the insufficient free volume in the solid state and the structural constraints of the macromolecular network.

The UV−vis absorption band of a 100 °C annealed **P(8)** film sample (nematic phase) is characterized by a

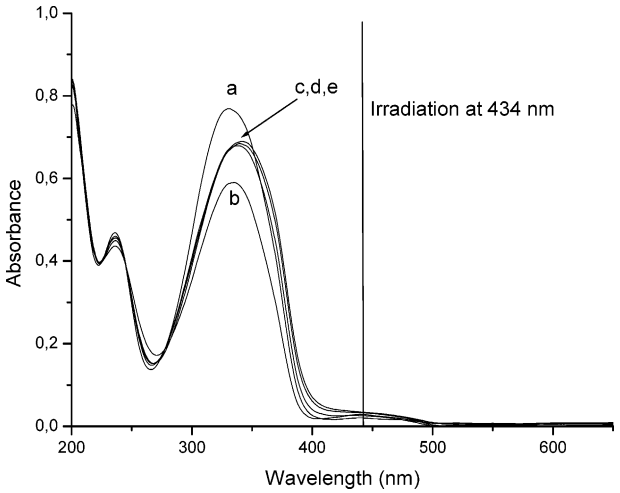

Figure 8. UV−visible spectra of **P(8)** film sample at 25 °C: (a) virgin isotropic film; (b) virgin isotropic film after 250 min irradiation at 366; (c−e) film from part b irradiated at 434 nm for 30, 60, and 130 min.

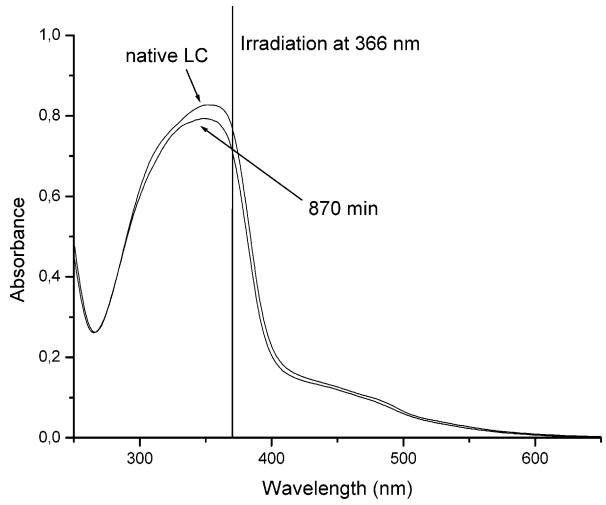

Figure 9. UV−visible spectra of **P(8)** film sample at 25 °C, previously annealed at 100 °C to show the nematic phase. The sample is exposed to UV irradiation at 366 nm for 870 min.

strong asymmetry, with a broadening at longer wavelength (Figure 9). This could be attributed to strong J-aggregations and to the strong dipolar interchain interactions, which predominate in the LC phase. When the LC polymeric film was exposed to UV irradiation at 366 nm for 870 min, as shown in Figure 9, only a little decrease of band intensity has been observed. The photostability, under these irradiation conditions, suggests that in the nematic phase the *trans*-azobenzene moieties are blocked in ordered domains and they have insufficient free volume to undergo the isomerization.

It is interesting to note that, after UV exposure, all polymer films were completely soluble in organic solvents as their native forms, which confirms that the allyl group is not reactive in photoisomerization conditions.

4. Conclusions

The molecule 4′-hydroxyphenyl(4-hydroxy-3-allyl)-azobenzene is mesogenic and it can be used for preparing PCLs, similarly to that reported for the allylbiphenol.[1] This is the result of the effect of side allyl group that destabilizes the crystalline phase and does not affect the nematic order. Moreover, for two polymers of the series, a pseudohexagonal molecular packing is observed with five to six chains allocated in the unit cell.

The UV−vis spectra in solution show that the synthesized polymers can undergo typical trans-to-cis and cis-to-trans photoisomerizations processes, under appropriate UV irradiation, with enhanced fatigue resistance response. The isomerization of azobenzene chromophores in the amorphous solid state is slower than in solutions, and it is inhibited in the nematic LC phase. This seems to be due to the presence of strong J-aggregation and molecular constraints, which reduce the free volume in the polymer matrix.

We will extend this study to the cross-linking process, involving the side allyl moiety, and its effect on the morphology induced on the samples. The effect of high power UV irradiation on the destabilization of nematic phase will be also investigated.

Acknowledgment. Support by FIRB "Micropolys" Project financed by the Ministero del'lIstruzione, dell'Università e della Ricerca (MIUR) and Consorzio INSTM is gratefully acknowledged.

References and Notes

(1) Acierno, D.; Fresa, R.; Iannelli, P.; Vacca, P. *Polymer* **2000**, *41*, 4179.
(2) Acierno, D.; Amendola, E.; Fresa, R.; Iannelli, P.; Vacca, P. *Polymer* **2000**, *41*, 7785.
(3) Angeloni, S.; Caretti, D.; Carlini, C.; Chiellini, E.; Galli, G.; Altomare, A.; Solaro, R. *Liq. Cryst.* **1989**, *4*, 513.
(4) Blumstein, A.; Thomas, O. *Macromolecules* **1982**, *15*, 1264.
(5) Hiruma, N.; Funaki, K.; Koide, N.; Iimura, K. *Rep. Prog. Polym. Phys. Jpn.* **1984**, *27*, 245.
(6) Rimura, K.; Koide, N.; Ohta, R. *Rep. Prog. Polym. Phys. Jpn.* **1981**, *24*, 231.
(7) Asrar, J.; Thomas, O.; Zhou, O.; Blumstein, A. *Proc. Macro-IUPAC*, Amherst, **1982.**
(8) Reck, B.; Ringsdorf, H. *Makromol. Chem. Rapid Commun.* **1985**, *6*, 291.
(9) Zentel, R.; Reckert, G. *Makromol. Chem.* **1986**, *187*, 1915.
(10) Voigt-Martin, I. G.; Durst, H.; Reck, B.; Ringsdorf, H. *Macromolecules* **1988**, *21*, 1620.
(11) Hall, H. K.; Kuo, T.; Lenz, R. W.; Leisle, T. M. *Macromolecules* **1987**, *20*, 2041.
(12) Srinivas, O.; Mitra, N.; Surolia, A.; Jayaraman, N. *J. Am. Chem. Soc.* **2002**, *124*, 2124.
(13) Hvilsted, S.; Andruzzi, F.; Kulinna, C.; Siesler, H. W.; Ramanujam, P. S. *Macromolecules* **1995**, *28*, 2172.
(14) Kurihara, S.; Yoneyama, D.; Nonaka, T. *Chem. Mater.* **2001**, *13*, 2807.
(15) Kurihara, S.; Sakamoto, A.; Nonaka, T. *Macromolecules* **1998**, *31*, 4648.
(16) Yamamoto, H.; Nishida, A. *Macromolecules* **1986**, *19*, 943.
(17) Yu, Y.; Nakano, M.; Ikeda, T. *Nature (London)* **2003**, *425*, 145.
(18) Jaffe, H. H.; Orchin, M. *Theory and Application of Ultraviolet Spectroscopy*; Wiley: New York, 1962.
(19) Altomare, A.; Carlini, C.; Ciardelli, F.; Solaro, R.; Houben, J. L.; Rosato, N. *Polymer* **1983**, *24*, 95.
(20) Fischer, E. *EPA Newsl.* **1984**, *21*, 33.
(21) Irie, M. *Photoresponsive Polymers*; Springer-Verlag: Berlin, 1982.
(22) Irie, M.; Suzuki, T. *Makromol. Chem., Rapid Commun.* **1987**, *8*, 607.
(23) Kumar, G. S.; Neckers, D. C. *Chem. Rev.* **1989**, *89*, 1915.
(24) Angiolini, L.; Caretti, D.; Giorgini, L.; Salatelli, E.; Altomare, A.; Carlini, C.; Solaro, R. *Polymer* **2000**, *41*, 4767.
(25) Irie, M.; Hayashi, K. *J. Macromol. Sci. Chem.* **1979**, *13*, 511.
(26) Irie, M.; Hirano, K.; Hashimoto, S.; Hayashi, K. *Macromolecules* **1981**, *14*, 262.
(27) Kumar, G. S.; DePra P.; Neckers, D. C. *Macromolecules* **1984**, *17*, 1912.
(28) Kumar, G. S.; DePra, P.; Zhang, K.; Neckers, D. C. *Macromolecules* **1985**, *18*, 2463.
(29) Shimomura, M.; Kunitake, T. *J. Am. Chem. Soc.* **1987**, *109*, 5175.

MA049319K